

On: 27 July 2007
Access Details: Free Access
Publisher: Taylor & Francis
Informa Ltd Registered in England and Wales Registered Number: 1072954
Registered office: Mortimer House, 37-41 Mortimer Street, London W1T 3JH, UK

Cover
not
available

Applied Occupational and Environmental Hygiene

Publication details, including instructions for authors and subscription information:
<http://oeh.informaworld.com/soeh/title~content=t713768777>

Detecting H⁺ in Ultrafine Ambient Aerosol Using Iron Nano-Film Detectors and Scanning Probe Microscopy

Beverly S. Cohen; Wei Li; Judy Q. Xiong; Morton Lippmann

Online Publication Date: 01 January 2000

To cite this Article: Cohen, Beverly S., Li, Wei, Xiong, Judy Q. and Lippmann, Morton (2000) 'Detecting H⁺ in Ultrafine Ambient Aerosol Using Iron Nano-Film Detectors and Scanning Probe Microscopy', Applied Occupational and Environmental Hygiene, 15:1, 80 - 89

To link to this article: DOI: 10.1080/104732200301881

URL: <http://dx.doi.org/10.1080/104732200301881>

PLEASE SCROLL DOWN FOR ARTICLE

The American Conference of Governmental Industrial Hygienists (<http://www.acgih.org/>) and the American Industrial Hygiene Association (<http://www.aiha.org/>) have licensed the Taylor & Francis Group to publish this article and other materials. To join the American Conference of Governmental Industrial Hygienists visit <http://www.acgih.org/Members/>. To join the American Industrial Hygiene Association visit <http://www.aiha.org/Content/BecomeMember/becomemember-splash.htm>.

Full terms and conditions of use: <http://oeh.informaworld.com/terms-and-conditions-of-access.pdf>

This article maybe used for research, teaching and private study purposes. Any substantial or systematic reproduction, re-distribution, re-selling, loan or sub-licensing, systematic supply or distribution in any form to anyone is expressly forbidden.

The publisher does not give any warranty express or implied or make any representation that the contents will be complete or accurate or up to date. The accuracy of any instructions, formulae and drug doses should be independently verified with primary sources. The publisher shall not be liable for any loss, actions, claims, proceedings, demand or costs or damages whatsoever or howsoever caused arising directly or indirectly in connection with or arising out of the use of this material.

© Taylor and Francis 2007

Detecting H⁺ in Ultrafine Ambient Aerosol Using Iron Nano-Film Detectors and Scanning Probe Microscopy

Beverly S. Cohen, Wei Li, Judy Q. Xiong, and Morton Lippmann

Nelson Institute of Environmental Medicine, New York University School of Medicine, Tuxedo, New York

Recent epidemiological evidence strongly suggests that ambient-particle-associated acidity is more closely correlated with total mortality and hospital admissions for respiratory disease than indices of total particulate mass. In addition, evidence is accumulating to support the hypothesis that the number of ultrafine ($d \leq 200$ nm) acid particles, rather than ambient mass, is an important determining factor affecting lung injury. Both outdoor and indoor air environments are dominated by nanometer-sized particles. However, no data are currently available on the size distribution or number concentration of acidic ambient ultrafine particles largely because there are no suitable methods for measuring these important quantities. We have developed a method to accomplish these measurements based on the use of iron nano-films for detection of acid droplets. Detectors were prepared by vapor deposition of iron onto 12-mm-diameter glass cover slips. The detectors develop reaction sites when exposed to H₂SO₄ or NH₄HSO₄ particles. Exposures to non-acidic particle (NaCl and [(NH₄)₂SO₄]) result in no detectable surface deformations. The nano-films are examined with scanning probe microscopy (SPM) for the enumeration of reaction sites. Until recently, direct visualization of individual objects smaller than 200 nm has been possible only with electron microscopy. The advancement of SPM provides the opportunity to examine the detector surface features with high quality three dimensional imaging.

Keywords Acidic Ultrafine Particles, Acidic Ambient Particles, Ultrafine Particles and Lung Injury, Ambient Aerosols, Iron Nano-Film Detectors, Ultrafine-Particle Number Concentration, Ultrafine-Particle Size Distribution, PM₁₀ and Respiratory Disease, Scanning Probe Microscopy

There is a growing body of epidemiological data indicating consistent and coherent associations between ambient par-

ticulate matter (PM) and excess mortality and morbidity. It is unlikely that all components of PM are equally toxic, and recent epidemiological evidence strongly suggests that ambient particle associated acidity is more closely correlated with total mortality than indices of total particulate mass^(1,2) and with hospital admissions for respiratory diseases.^(3,4) In addition, evidence is accumulating to support the hypothesis that the number of acid particles is an important determining factor affecting lung injury.^(5–10) If this hypothesis is correct, the number of acid-containing particles that deposit per unit surface of the epithelial lining of human respiratory system may be a significantly more important determinant of the risk of morbidity and mortality than the total mass deposited at common ambient levels. However, no data are available on the size distribution or number concentration of acidic ambient ultrafine particles largely because there have been no suitable methods for measuring these important quantities. This article briefly reviews some of the evidence for adverse health effects of PM and the data that suggest a particular role for ultrafine acid particles, and presents our recent progress on the development of a method to determine the number concentration of ultrafine ambient acid particles. The method utilizes ultra-thin metal detector films that will form reaction pits when an acidic particle is deposited on the film, and scanning probe microscopy to visualize and quantify the reaction sites. The report is of our early characterization of the detectors and the image analysis system.

BACKGROUND

Health Effects of PM

When other known risk factors have been taken into account in regression analyses, it has been possible to show that daily changes of PM are associated with changes in daily mortality;^(11–21) hospital admissions for respiratory diseases;^(3, 4, 22–27) and emergency room visits for respiratory diseases,^(17, 28, 29) respiratory symptoms,^(14, 23, 30–34) and lung

function.^(14,23,31,32,34-37) For these various responses, there is sometimes a lag of one to a few days between exposure and response.

Differences in long-term average levels of PM pollution have been associated with differences in annual mortality rates,⁽³⁸⁻⁴¹⁾ the prevalence of chronic disease and symptoms,⁽⁴²⁻⁴⁵⁾ lost time from work or school,⁽⁴⁶⁻⁵⁰⁾ and reduced lung function baselines.^(43,51-53) When multiple regressions are performed which include pollutant vapors as well as PM, the PM variable tends to be most influential.^(13,42,43,48,49,54,55) The only exceptions appear to be hospital admissions and symptoms,^(3,4,18,25) where ozone (O₃) is sometimes as, or more, influential on the regressions than PM.

Airborne PM concentrations have generally been expressed in terms of mass concentration per unit volume (e.g., $\mu\text{g}/\text{m}^3$), as determined by dividing the mass accumulated in a sampling substrate (such as a filter disc or sheet) by the volume of air from which the particles were extracted. The sampled mass is often dominated by the largest particles that reach the collector. Thus, the concentration of total suspended particulate matter (TSP) is numerically larger than that for PM₁₀ (thoracic particulate matter with aerodynamic diameters below 10 μm), which, in turn, is larger than that for PM_{2.5} (fine particulate matter with aerodynamic diameters below 2.5 μm). The PM_{2.5} contains the accumulation mode of the atmospheric aerosol (which extends from 2.5 μm down to ~ 100 nm). This mode includes most of the mass of the secondary aerosols formed in the atmosphere from gaseous pollutant precursors by chemical reactions, including sulfuric acid and its ammonium salts, ammonium nitrate, and photochemically formed organics. The PM_{2.5} fraction also includes the transient, rapidly coagulating ultrafine aerosol mode, which extends from ~ 100 nm down to ~ 10 nm, but the mass of this mode makes little contribution to the overall mass of the PM_{2.5}. On the other hand, in terms of the number concentration of the ambient aerosol, the ultrafine mode is dominant.

Acid Aerosols

In some studies that have utilized multiple PM metrics in their regression analyses, the strength of association improves as one goes from TSP to PM₁₀ to PM_{2.5} to SO₄⁻, the latter being primarily within the PM_{2.5} fraction of the aerosol.^(4,56) Based on extrapolation of the associations between annual mortality and SO₄⁻ concentrations in 98 U.S. communities, which showed nonsignificant associations with TSP and PM₁₀, and significant associations with PM_{2.5} ($p < 0.01$) and SO₄⁻ ($p < 0.001$), Lippmann⁽⁵⁷⁾ hypothesized that had H⁺ been measured, the effect coefficient would be larger and the p value smaller.

Sulfuric acid and ammonium bisulfate, both strongly acidic, are important components of the fine and ultrafine particle modes in the ambient atmosphere. Recent reports have observed that ambient hydrogen and sulfate ion concentrations have significant associations with adverse health effects.^(2,4,58,59) Investigators who have included strong acidity measurements in their

monitoring of the ambient atmosphere have found that acidity is significantly correlated with adverse health effects.^(4,43,60,61) Acidity also had a strong correlation with the prevalence of bronchitic symptoms and lung function in children.^(62,63) Additionally, Thurston and colleagues observed that acidity had the highest relative particle metric strength of association with respiratory and asthma admissions in Toronto.⁽⁴⁾

Ambient acidic sulfates may exist in two forms: acid dissolved in aqueous droplets and as a surface layer on solid particles. The first type of aerosol has been studied extensively in animal and controlled clinical studies. The second type of aerosol is formed by sulfuric acid adsorption onto or formation on particles with large surface to volume ratio, such as the typical carbonaceous or fly ash particle, and is very potent in altering various indices of response. Although sulfuric acid droplets have been found to produce alterations in a number of aspects of pulmonary physiology, biochemistry, and structure in clinical studies,⁽⁶⁴⁾ the only effect observed in healthy volunteers at concentrations relevant to ambient exposures is altered mucociliary particle clearance from the lungs of nonsmoking adults.^(65,66) The only other adverse effects occurring at concentrations approaching environmental levels have been pulmonary mechanics changes in asthmatic subjects.⁽⁶⁷⁻⁶⁹⁾ To date, clinical work studying acid aerosols has not reported significant adverse effects and, thus, a controversy surrounds the plausibility of the association of acid aerosols with adverse health effects in epidemiological studies.⁽⁵⁾

Number of Acid Particles

Chen et al.⁽⁶⁾ provided important evidence regarding the role of acid particle number in cellular response. Guinea pigs were exposed to varying amounts of sulfuric acid layered onto 10⁸ ultrafine carbon core particles, and to a constant (300 $\mu\text{g}/\text{m}^3$) concentration of sulfuric acid layered onto 10⁶, 10⁷, or 10⁸ particles. All of these particles had diameters of approximately 90 nm, the acid being adsorbed onto carbon core particles. Indicators of irritant potency on macrophages harvested from the lungs of exposed animals clearly showed an increased response to a constant dose of acid when it was divided into an increased number of particles, as well as a response to increased dose of acid at a constant number concentration. Early work by Amdur and Chen⁽⁵⁾ suggested that number concentration was important for sulfuric acid aerosol, and Hattis et al.^(9,10) gave the concept a name, "irritation signaling." The subsequent research of Chen et al.⁽⁶⁾ indicated that inhaled acid-coated particles much smaller than those discussed by Hattis et al.^(9,10) were capable of producing lung responses. Evidence, some of which was noted above, has begun to accumulate to support the hypothesis that the number of ultrafine particles that deposit per unit surface of the epithelial lining of human respiratory system is an important determining factor affecting lung injury,^(5-10,70) and that the resulting alveolar inflammation is able to provoke attacks of acute respiratory illness in susceptible individuals.⁽⁸⁾ In particular, the

work of Peters et al.^(70,71) suggested that at ambient levels, the number concentration of inhaled particles may be a significantly more important determinant of the risk than inhaled mass measures. They report that the best correlation for decrement in peak expiratory flow-rate (PEF) measured in 27 adults with a history of asthma was with the number concentration of particles with diameters between 10 and 100 nm.⁽⁷⁰⁾

This is important because both outdoor⁽⁶⁴⁾ and indoor⁽⁷²⁻⁷⁴⁾ air environments are dominated by nanometer-sized particles, but they are difficult to isolate based on mass measurements. It has been suggested that the responses to PM cannot be associated with number concentration because the number does not always correlate with PM_{2.5}. However, the Environmental Protection Agency (EPA) has concluded that a correlation between the total number and total fine particle mass might be expected if comparisons were made over periods of days.⁽⁶⁴⁾

We have developed a method to measure the size distribution and number concentration of acidic ambient ultrafine particles. Based on a method reported by Horstman and Wagman⁽⁷⁵⁾ for much larger particles, it utilizes thin iron-coated detectors on which reaction pits are formed when the film is exposed to acidic particles. A future report will detail the sampling system being developed for deployment of these detectors.

METHODS

Detectors

Iron nano-film detectors 25, 50, 100, and 200 nm thick, were prepared by vapor deposition onto 12-mm-diameter glass cover slips by a commercial vendor (IBM Corporation, Yorktown Heights, NY).

Test Aerosols

Three different generators were used to produce: (1) micrometer-sized test particles; (2) nanometer-size range particles; and (3) acid-coated carbon particles.

Initial characterization of the iron nano-film on glass-substrate detectors utilized sulfuric acid droplets of about 1 micrometer in diameter with geometric standard deviations (GSD) of 1.1-1.2 generated with a vibrating orifice generator (VOAG Model 3450 TSI, St. Paul, MN). Monodisperse NaCl, NH₄SO₄ and (NH₄)₂SO₄ particles were also generated with the VOAG.

Nanometer-sized calibration droplets were generated with a condensation H₂SO₄ aerosol generation system developed in our laboratory.⁽⁷⁶⁾ Pre-heated particle-free air passes over the surface of sulfuric acid heated in a thermostated bath. The mixture of air and sulfuric acid vapor then passes through a thermostated water-cooled condenser to form a nearly monodisperse aerosol. The particle size can be controlled by varying the evaporating temperature of the liquid H₂SO₄ and the carrier gas flow rate. The generator has a very stable output with regard to particle size with an average relative SD less than 0.03 over a time scale of six hours. The generated aerosol is classified by the first

differential mobility analyzer (DMA Model 3071 TSI, St. Paul, MN) of a Tandem DMA system under the same relative humidity (RH) conditions. The size and concentration of the aerosol can be monitored by the second DMA and a condensation particle counter (CPC, Model 3010S, TSI St. Paul, MN) equipped with a scanning electrical mobility spectrometer chip and software (SEMS Model 390089, TSI, St. Paul, MN).

Additional tests used ultrafine carbon particles approximately 26, 60, and 100 nm in diameter onto which H₂SO₄ vapor is deposited. These were produced in a condensation furnace generator as described by Chen et al.⁽⁶⁾ In this system, a high-temperature silicon carbide furnace is maintained at 1098°C. A small quantity of acetylene in Ar (1% by volume) is introduced into a quartz tube in the furnace. At high temperatures, without sufficient oxygen to permit combustion, the acetylene undergoes thermal decomposition, and produces ultrafine carbon particles. The carbon particles are diluted immediately with one or two ejector dilutors and mixed with sulfuric acid droplets in a quartz tube maintained at 500°C. Sulfuric acid undergoes an evaporation, then a condensation process in a water-cooled condenser to form a thin layer of sulfuric acid on the carbon particles.

Test particles were deposited onto the detectors with an Electrostatic Aerosol Sampler (EAS, Model 3100, TSI, Inc., St. Paul, MN). The sampling time was controlled to produce a surface number concentration about five particles per 10,000 square micrometer on the detectors.

Analysis

Deposition of acid droplets onto the nano-films results in reaction spots that can be examined by optical microscopy (OM), scanning electron microscopy (SEM), transmission electron microscopy (TEM), or scanning probe microscopy (SPM). The amount of surface area that can be scanned is severely limited for the latter three techniques so that uniform deposition onto the substrates is needed.

The uniformity of deposition was examined using 2- μ m-diameter NaCl particles deposited onto the uncoated substrate (glass cover slips). The deposited particles were examined with OM. Statistical analysis of particle surface density indicated random deposition.

The resolution of optical microscopes is not sufficient for examining the nanometer-sized features that result from the interaction of the ultrafine acid aerosols with the iron films. They can be detected by SEM or TEM, both of which require special sample preparation. Samples for analysis must be either collected, or mounted, on conducting stubs for SEM, and on fragile electron transparent substrates for TEM. In addition, scanning must be done in vacuum, which is inconvenient and time-consuming. When particles deposited on the detectors are examined with EM loss of volatile components may occur because of the vacuum. Artifacts may also result from vaporization of very small particles as they are scanned by the highly concentrated electron beam. Samples are usually coated for SEM analysis to provide

a conducting surface to avoid charge buildup and beam distortions, but coating is not necessary for the iron nano-films.

Scanning Probe Microscopy

Until recently, direct visualization of individual particles smaller than 200 nm has been possible only with electron microscopy. The advancement of SPM provides the opportunity to examine particles in the ultrafine size range with high-quality three-dimensional imaging. SPM is superior to SEM or TEM because it is relatively inexpensive, requires little sample treatment, and can be performed at ambient pressure. Also the depth of field of SPM is superior to that of TEM and the resolution is superior to SEM.

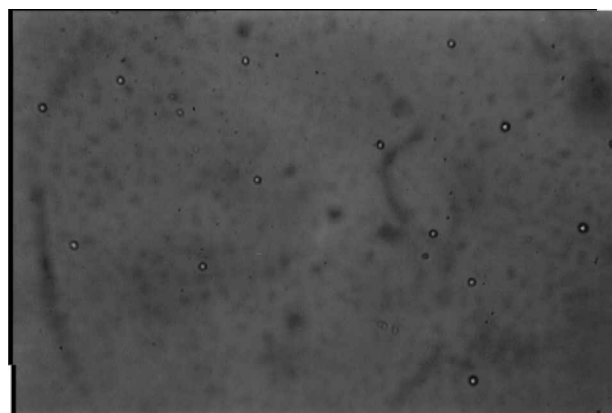
Scanning probe microscopy (SPM) is a collective term for a family of microscopes that includes scanning tunneling microscopy (STM), atomic force microscopy (AFM), magnetic force microscopy (MFM), lateral force microscopy (LFM), and so on. This new generation of microscopes was inspired by the invention of STM,⁽⁷⁷⁾ after which many improvements have been made. The applications of SPM range from examination of DNA structures in biological studies to surface examination of wafers in the semiconductor industry.

In initial tests we examined samples by both SEM and SPM. Subsequent samples were all examined by SPM. We used atomic force microscopy (AFM), a form of SPM (AutoProbe CP, Park Scientific Instruments, Sunnyvale, CA). The operation of this microscope has been detailed by Howland and Benatar⁽⁷⁸⁾ and a brief description follows.

In AFM a surface is sensed via a sharp probe tip a few micrometers long and less than 10 nm in diameter. The tip is held by a low spring-constant cantilever mounted on a coarse mechanical positioning system. A sample stub mounted on a piezoelectric scanner moves the sample under the probe tip. The deflection of the probe cantilever, which is a reflection of the surface roughness, is detected by a position-sensitive photodetector. The signal is then processed by computer to show the scanned surface image on a screen. A resolution of a few nanometers can be easily achieved for both vertical and horizontal scans.

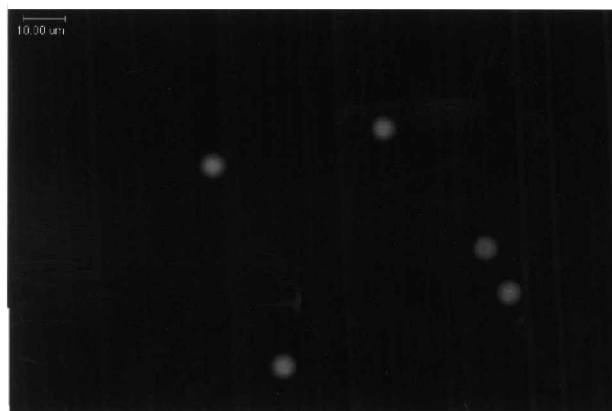
Three modes of operation have been developed for surface characterization by AFM—contact mode, non-contact mode, and intermittent-contact mode. Each was tested for these detectors, but most of the work was carried out in contact mode.

The contact mode was the first AFM operating mode developed. In contact AFM mode, a tip is held above the sample within the repulsive van der Waals force range, making “physical contact” with the sample. Because the spring constant of the cantilever is smaller than the intermolecular force, the physical contact does not cause significant damage to the surface. Therefore, deformation of the cantilever reflects the surface features of the sample. Besides the van der Waals force, a capillary force exists when operating at ambient conditions because a thin water layer is absorbed on sample surfaces. However, the capillary



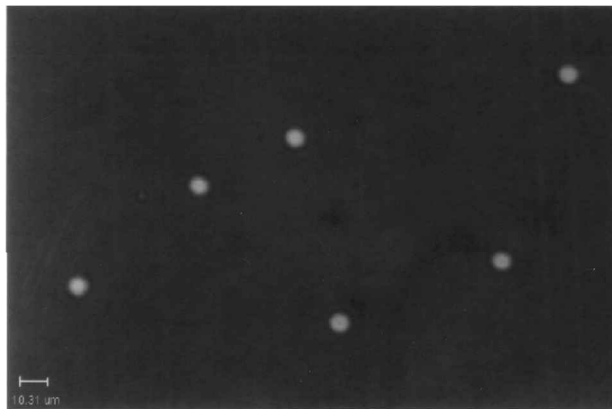
1.13 μm H₂SO₄ on cover glass

(a)



1.1 μm H₂SO₄ on 25-nm film

(b)



1.2 μm NH₄HSO₄ on 25-nm film

(c)

FIGURE 1

Reaction sites viewed by OM: (a) Acid particles deposited on glass cover slip; (b) H₂SO₄ particles on 25-nm iron nano-film; (c) NH₄HSO₄ particles on 25-nm iron nano-film.

force should be constant as long as the tip is in contact with the sample and the water layer is homogeneous within the scan range.

The interaction force between the tip and sample surface in the contact mode is the strongest among three AFM operation modes. In developing the AFM method for studying acid particles, we found that a foreign particle on substrate can be distinguished from the roughness of the substrate because it can be moved by the probe tip. It may appear as a linear smear on the image, or simply be pushed to the end of the scan line.

Non-contact AFM is one of several vibrating cantilever techniques in which the cantilever is vibrated near the surface of the sample. The space between the tip and the sample is on the order of tens to hundreds of angstroms (attractive van der Waals force range). The system vibrates the cantilever near its resonant frequency and detects changes in the frequency when the tip comes near the sample surface.

The third type of AFM is intermittent mode which is similar to non-contact, except that for intermittent AFM the probe tip is brought closer to the sample so that at the bottom of its oscillation cycle it barely hits or taps the sample. The intermittent AFM is advantageous in cases when the surface is likely to be damaged by the lateral force of the scanning probe in contact mode.

RESULTS AND DISCUSSION

When unexposed detectors are examined by OM less than three holes per square millimeter are visible. When detectors exposed to acid particles with diameters of about $1.0\ \mu\text{m}$ are similarly examined, clear circular areas are observed that appeared to be reaction pits, with each droplet producing one spot (Figure 1). Spot diameters were 8.4 ± 3.4 , 8.7 ± 4.2 , 5.9 ± 2.7 , and $4.3 \pm 3.2\ \mu\text{m}$ (mean \pm SD) for detector thickness of 25, 50, 100, and 200 nm, respectively. The reaction areas had a much broader distribution than the original aerosol (Figure 2). Exposures to NaCl and $(\text{NH}_4)_2\text{SO}_4$ particles resulted in no detectable surface deformations by OM, while NH_4HSO_4 particles produced "pits" with diameters approximately the same as those from exposure to H_2SO_4 particles (Figure 1c). Thus, the detector is capable of distinguishing the strong acid aerosols from the completely neutralized aerosols.

Exploratory SPM scans of the blank nano-films were carried out to enable us to recognize the normal surface on the nanometer scale and to establish the number of visible features on the surface of an unexposed film. The surface roughness of the nano-films is about $\pm 1.8\ \text{nm}$ (Figure 3). This allows resolution of reactions sites that produce height deformations greater than about 6 nm. Scan parameters were established based on a trade-off

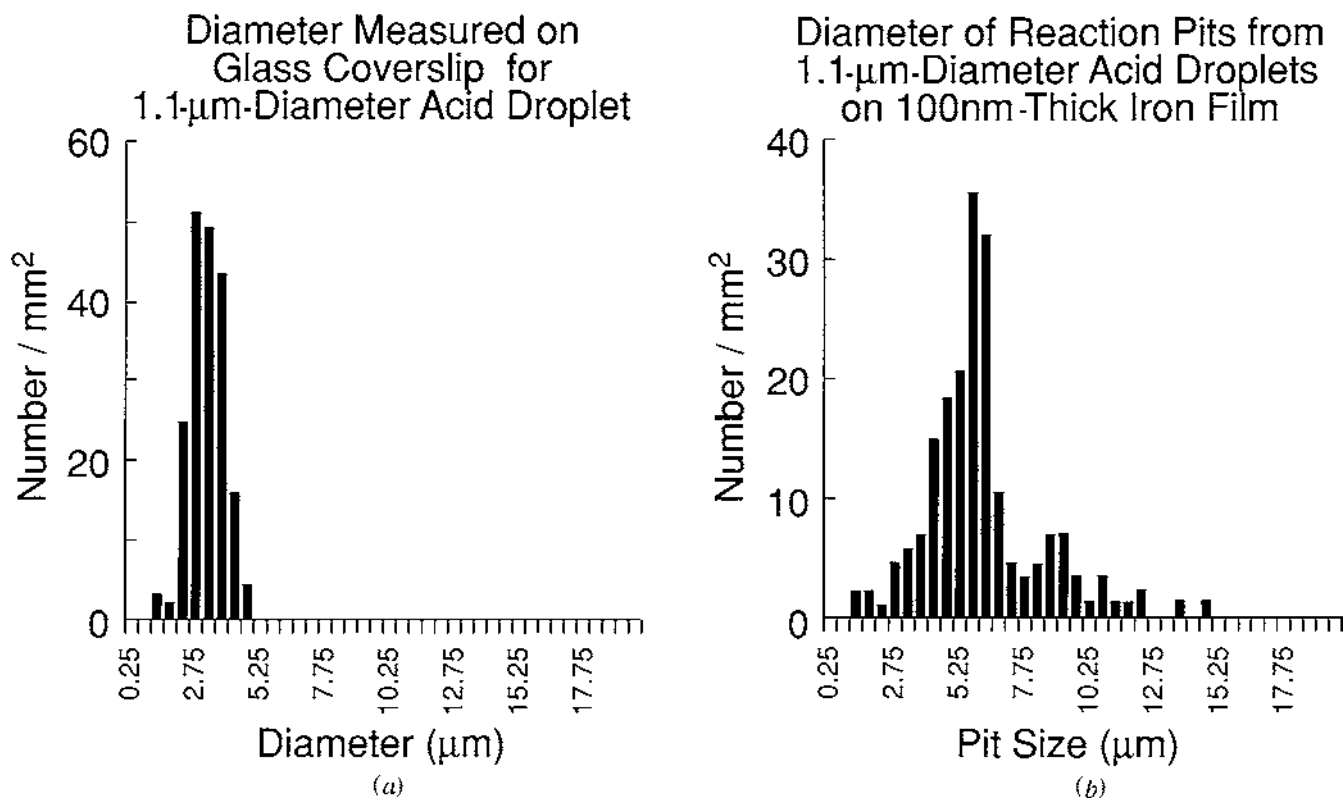
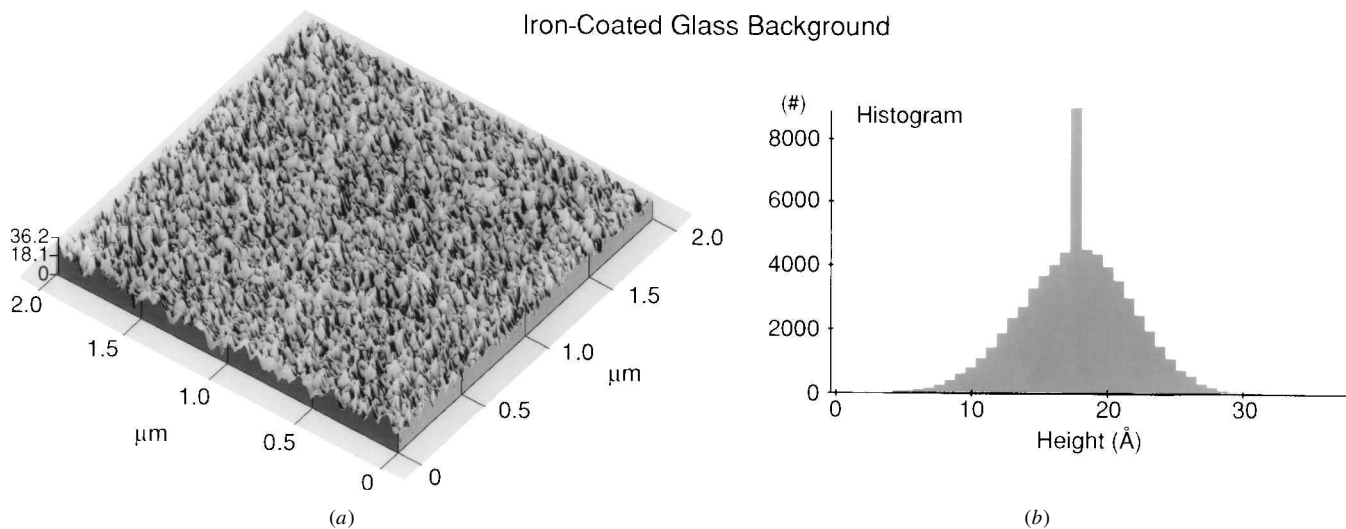


FIGURE 2

Size distribution of: (a) 1.1- μm -diameter acid particles deposited on glass; (b) reaction sites of the same particles on 100-nm-thick iron nano-film.

**FIGURE 3**

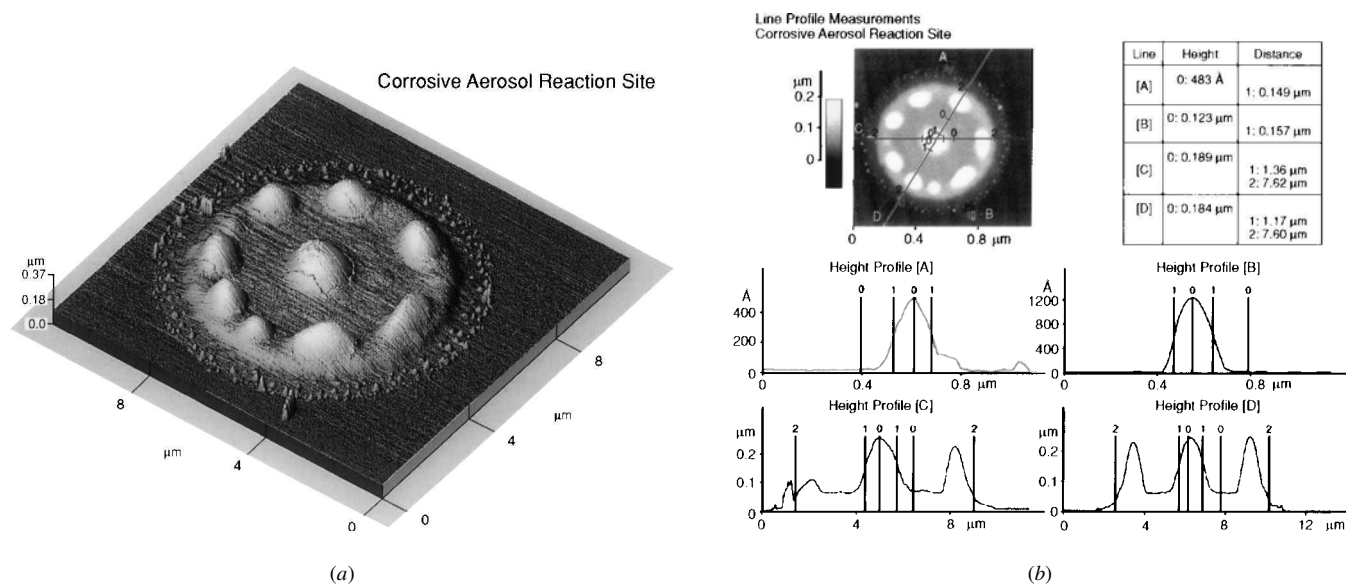
(a) SFM image of unexposed iron nano-film surface; (b) Histogram of height of surface features.

between total scan area, resolution, and scan duration for an individual detector. Scans of 16 randomly chosen, $10\ \mu\text{m} \times 10\ \mu\text{m}$ fields per detector at 512 pixels per line (19 nm/pixel) were selected. With these parameters, using acid droplet volume, film thickness and the measured ratio of droplet diameter to reaction site as a guide, a 20-nm acid droplet would produce a clearly detectable reaction site of approximately 100 nm on a 25-nm-thick detector film. With these scan parameters a mean of 0.25 visible spots per $10\ \mu\text{m} \times 10\ \mu\text{m}$ field was determined for blank detectors.

Following exposure to 20–50 nm acid particles the detectors were examined with both SEM and SPM. The surface texture at

the reaction sites appears to be unaltered as compared with the unreacted surface. Thus detection of reaction sites with SEM was very difficult due to the lack of contrast on the acid reacted spots.

By contrast, the reaction sites were clearly visualized with SPM. SPM revealed that the observed spots were actually bumps rather than the expected “pits” in the iron nano-film surface (Figures 4 and 5). The acid reaction with the nano-film caused a surface deformation, so that the entire surface looks the same except for the deformation. This is the reason why observation is so difficult with SEM; if a deformation is not elevated enough to produce a significant shadow at the viewing angle it is very hard

**FIGURE 4**

(a) Three-dimensional image of a reaction spot that resulted from depositing a 1.2- μm sulfuric acid particle on a 25-nm iron film; (b) detailed measurements on the reaction site shown in Figure 4A (see text).

Line Profile Measurements
48nm H₂SO₄ Droplets
(Sample 25-7)
Topography, 0916S01B.HDF

48nm H₂SO₄ Droplets
(Sample 25-7)
Topography, 0916S01B.HDF

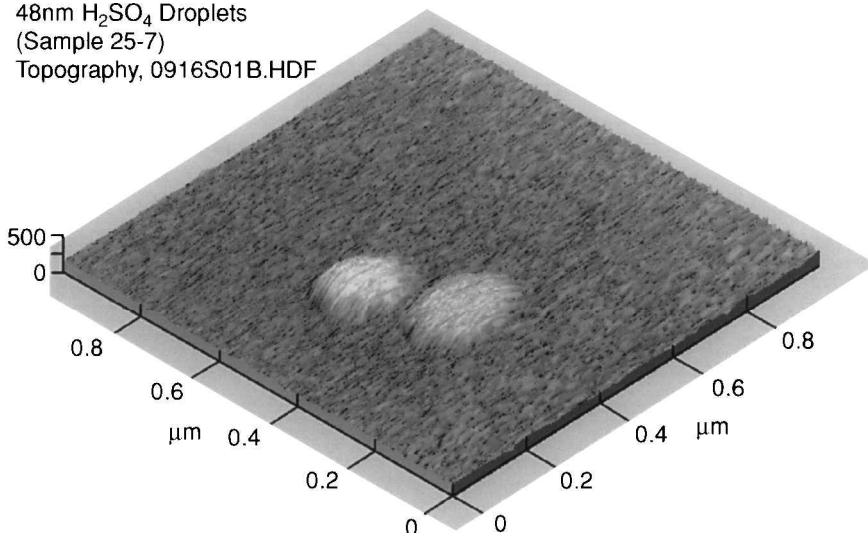
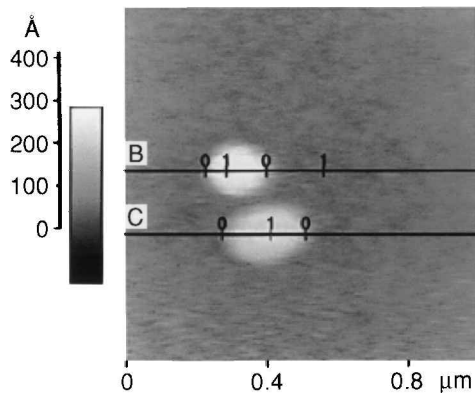


FIGURE 5

Reaction sites of two 48-nm H₂SO₄-droplets deposited on a 25-nm-thick iron film. Both 3D and top-view images are shown.

to discern. With SEM we could rarely see surface deformations less than 50 nm. In contrast, SPM is designed to easily detect angstrom scale elevations. SPM is also much simpler to use because little sample preparation is required, and it does not require a vacuum. Also, the principle of operation of the AFM and the data acquisition software used with our microscope (Proscan, Park Scientific, Sunnyvale, CA) allows excellent quantification

of three-dimensional size. Furthermore, there is a large sample support stage for enumeration of particles deposited over a wide surface area.

Figure 4 shows some of the output available with the SFM and data analysis system. Figure 4A shows the three-dimensional (3D) image of a reaction spot that resulted from depositing a 1.3- μ m sulfuric acid particle on a 25-nm iron nano-film. The

100nm H₂SO₄-Carbon Particles
(Sample 25-11)
Topography, 0717S007.HDF

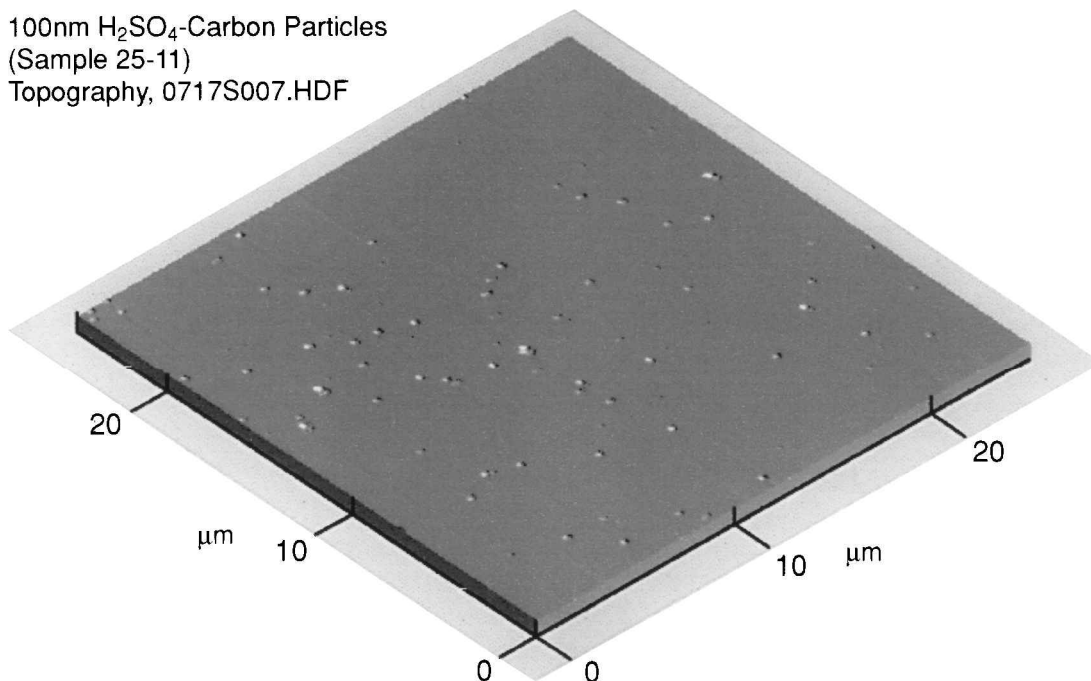


FIGURE 6

3D image of 100-nm H₂SO₄-carbon particles deposited on a 25-nm-thick iron film. Note the narrow size distribution of the calibration particles.

reaction site appears circular and has one large bump in the center surrounded by eight smaller bumps. The entire circular spot is raised and surrounded by many satellite extrusions. The mechanism that caused this appearance is still under investigation but it is likely that the collection mechanism used for this experiment (electrostatic precipitation) caused the large droplet to shatter.

Figure 4B shows detailed measurements on the reaction site shown in Figure 4A. Four profiles have been measured as shown in the top-view image. Profile A is located on top of the figure. It shows the height (height is expressed as above the surrounding area) and diameter (taken as width at half maximum) of one satellite bump: 48.3 nm and 149 nm, respectively. Profile B is located near the lower-right section. It is also of a satellite bump whose height and diameter are 123 nm and 157 nm, respectively. Profiles C and D are horizontal and diagonal scans across the reaction spots as shown in the top-view image. Images 3, 4A, and 4B were provided by Dr. C. Mooney of Park Scientific Instruments.

Extensive measurements were done for acid-coated carbon particles (13% of mass was acid) with diameter of 100 nm and geometric standard deviation of 1.4, collected on the 25-nm detectors. The nano-films were examined with non-contact SPM (Figure 6). As for the larger particles, deposition was very uniform. Heights and diameters were measured using the Proscan analysis program. The average height and standard deviation for 603 sites was 35 ± 16 nm and the average diameter was 704 ± 230 nm. Considering the size of the particles the variability is remarkably small. The reaction site to particle diameter ratios are similar to those obtained with droplets of pure sulfuric acid with diameters of 1.3 μ m.

To determine the ambient concentration of strong acid particles as a function of size using the images from these detectors requires additional knowledge. These are: (1) the ratio of the particle size to the size of the measured reaction site, and (2) the efficiency with which particles of a specific size are deposited onto the detectors (DE). For the former, calibration aerosols of different sizes and acid concentrations are deposited onto the detectors and the reaction sites evaluated for more detailed determination of the ratios of particle size to reaction site size. Tests to acquire sufficient information are ongoing. For the second, deposition efficiency (DE) depends on the sampling system. DE as a function of particle size is separately determined for each system using monodisperse fluorescein calibration aerosols. Further developmental work is in progress on samplers, and sampling systems, that allow accurate determination of the airborne concentration of strong acids using these nanofilm detectors.

SUMMARY AND CONCLUSIONS

To our knowledge, the detection system described here is the first reported method that can select ultrafine particles of an individual chemical species method for enumeration. The method uses nano-film iron detectors with which reaction sites are produced when acid deposits onto the films. One reaction site

results for each acid droplet. Surface scans with SPM allow enumeration as well as size analysis of the reaction sites produced when ultrafine acid-containing particles are deposited. Current studies are underway on the effects of detector storage, and on mechanisms for distinguishing extraneous particles. The latter is a substantial problem for ambient sampling, but in the contact AFM mode particles can be removed from the surface by repeated scans. Nonetheless, additional experiments are underway to distinguish and identify collected particles as well as acid reaction sites. These detectors are being incorporated into field samplers and also into a personal monitor for the evaluation of individual exposure to ultrafine acid aerosols.

ACKNOWLEDGMENTS

The authors thank the personnel of Park Scientific Instruments, Sunnyvale, California, in particular Dr. Chuck Mooney, Mr. Kirby Jensen, and Mr. David Campbell for their generous technical and operational assistance.

This work is supported by Environmental Protection Agency, Grant #R824791010, and is part of a center program supported by NIEHS Grant No. ES00260.

REFERENCES

1. Thurston, G.D.; Ito, K.; Lippmann, M.; et al.: Re-examination of London Mortality in Relation to Exposure to Acidic Aerosols During 1962–1973 Winters. *Environ Health Perspect* 79:73–82 (1989).
2. Lippmann, M.; Thurston, G.D.: Sulfate Concentrations as an Indicator of Ambient Particulate Matter Air Pollution for Health Risk Evaluations. *J Expos Anal Environ Epidemiol* 6(2):123–146 (1996).
3. Thurston, G.D.; Ito, K.; Kinney, P.L.; et al.: A Multi-Year Study of Air Pollution and Respiratory Hospital Admissions in Three New York State Metropolitan Areas: Results for 1988 and 1989 Summers. *J Expos Anal Environ Epidemiol* 2:429–450 (1992).
4. Thurston, G.D.; Ito, K.; Hayes, C.G.; et al.: Respiratory Hospital Admissions and Summertime Haze Air Pollution in Toronto, Ontario: Consideration of the Role of Acid Aerosols. *Environ Res* 65:271–290 (1994).
5. Amdur, M.O.; Chen, L.C.: Furnace-Generated Acid Aerosols: Speciation and Pulmonary Effects. *Environ Health Perspect* 79:147–150 (1989).
6. Chen, L.C.; Wu, C.Y.; Qu, Q.S.; et al.: Number Concentration and Mass Concentration as Determinants of Biological Response to Inhaled Irritant Particles. *Inhal Toxicol* 7:577–588 (1995).
7. Oberdorster, G.; Gelein, R.M.; Ferin, J.; et al.: Association of Particulate Air Pollution and Acute Mortality: Involvement of Ultrafine Particles. *Inhal Toxicol* 7:111–124 (1995).
8. Seaton, A.W.; MacNee, K.; Donaldson, D.; et al.: Particulate Air Pollution and Acute Health Effects. *Lancet* 345:176–178 (1995).
9. Hattis, D.; Wasson, J.M.; Page, G.S.; et al.: Acid Particles and the Tracheobronchial Region of the Respiratory System—An “Irritation-Signaling” Model for Possible Health Effects. *J Air Pollut Control Assoc* 37:1060–1066 (1987).
10. Hattis, D.S.; Abdollahzadeh, S.; Franklin, C.A.: Strategies for Testing the “Irritation-Signaling” Model for Chronic Lung Effects

- of Fine Acid Particles. *J Air Waste Manage Assoc* 40:322–330 (1990).
11. Fairley, D.: The Relationship of Daily Mortality to Suspended Particulates in Santa Clara County, 1980–1986. *Environ Health Perspect* 89:159–168 (1990).
 12. Schwartz, J.: Particulate Air Pollution and Daily Mortality in Detroit. *Environ Res* 56:204–213 (1991).
 13. Dockery, D.W.; Schwartz, J.; Spengler, J.D.: Air Pollution and Daily Mortality: Associations with Particulates and Acid Aerosols. *Environ Res* 59:362–373 (1992).
 14. Pope, III, C.A.; Dockery, D.W.: Acute Health Effects of PM-10 Pollution on Symptomatic and Asymptomatic Children. *Am Rev Respir Dis* 145:1123–1128 (1992).
 15. Schwartz, J.; Dockery, D.W.: Increased Mortality in Philadelphia Associated with Daily Air Pollution Concentrations. *Am Rev Respir Dis* 145:600–604 (1992).
 16. Schwartz, J.; Dockery, D.W.: Particulate Air Pollution and Daily Mortality in Steubenville, Ohio. *Am J Epidemiol* 135:12–19 (1992).
 17. Schwartz, J.: Air Pollution and Daily Mortality in Birmingham, Alabama. *Am J Epidemiol* 137:1136–1147 (1993).
 18. Schwartz, J.: Air Pollution and Hospital Admissions for the Elderly in Birmingham, Alabama. *Am J Epidemiol* 139:589–590 (1994).
 19. Saldiva, P.H.N.; Pope, III, C.A.; Schwartz, J.; et al.: Air Pollution and Mortality in Elderly People: A Time Series Study in Sao Paulo, Brazil. *Arch Environ Health* 50:159–163 (1995).
 20. Kinney, P.L.; Ito, K.; Thurston, G.D.: A Sensitivity Analysis of Mortality/PM-10 Associations in Los Angeles. *Inhal Toxicol* 7:59–69 (1995).
 21. Ito, K.; Kinney, P.L.; Thurston, G.D.: Variations in PM₁₀ Concentrations Within Two Metropolitan Areas and Their Implications to Health Effects Analyses. *Inhal Toxicol* 7:735–745 (1995).
 22. Pope, III, C.A.: Respiratory Disease Associated with Community Air Pollution and a Steel Mill, Utah Valley. *Am J Public Health* 79:623–628 (1989).
 23. Pope, III, C.A.: Respiratory Hospital Admissions Associated with PM-10 Pollution in Utah, Salt Lake, and Cache Valleys. *Arch Environ Health* 46:90–97 (1991).
 24. Lipfert, F.W.; Hammerstrom, T.: Temporal Patterns in Air Pollution and Hospital Admissions. *Environ Res* 59:374–399 (1992).
 25. Burnett, R.T.; Dales, R.E.; Raizenne, M.E.; et al.: Effects of Low Ambient Levels of Ozone and Sulfates on the Frequency of Respiratory Admissions to Ontario Hospitals. *Environ Res* 65:172–194 (1994).
 26. Schwartz, J.: Particulate Air Pollution and Chronic Respiratory Disease. *Environ Res* 62:7–13 (1994).
 27. Delfino, R.J.; Becklake, M.R.; Hanley, J.A.: The Relationship of Urgent Hospital Admissions for Respiratory Illnesses to Photochemical Air Pollution Levels in Montreal. *Environ Res* 67:1–19 (1994).
 28. Samet, J.M.; Speizer, F.E.; Bishop, Y.; et al.: The Relationship Between Air Pollution and Emergency Room Visits in an Industrial Community. *J Air Pollut Control Assoc* 31:236–240 (1981).
 29. Sunyer, J.; Saez, M.; Murillo, C.; et al.: Air Pollution and Emergency Room Admissions for Chronic Obstructive Pulmonary Disease: A 5-Year Study. *Am J Epidemiol* 137:701–705 (1993).
 30. Braun-Fahrlander, C.; Ackermann-Leibrich, U.; Schwartz, J.; et al.: Air Pollution and Respiratory Symptoms in Preschool Children. *Am Rev Respir Dis* 145:42–47 (1992).
 31. Hoek, G.; Brunekreef, B.: Acute Effects of a Winter Air Pollution Episode on Pulmonary Function and Respiratory Symptoms of Children. *Arch Environ Health* 48:328–335 (1993).
 32. Hoek, G.; Brunekreef, B.: Effects of Low Level Winter Air Pollution Concentrations on Respiratory Health of Dutch Children. *Environ Res* 64:136–150 (1994).
 33. Ostro, B.D.; Lipsett, M.J.; Mann, J.K.; et al.: Air Pollution and Respiratory Morbidity Among Adults in Southern California. *Am J Epidemiol* 137:691–700 (1993).
 34. Roemer, W.; Hoek, G.; Brunekreef, B.: Effect of Ambient Winter Air Pollution on Respiratory Health of Children with Chronic Respiratory Symptoms. *Am Rev Respir Dis* 147:118–124 (1993).
 35. Dockery, D.W.; Ware, J.H.; Ferris, Jr., B.G.; et al.: Change in Pulmonary Function in Children Associated with Air Pollution Episodes. *J Air Pollut Control Assoc* 32:937–942 (1982).
 36. Pope, III, C.A.; Kanner, R.E.: Acute Effects of PM-10 Pollution on Pulmonary Function of Smokers with Mild to Moderate Chronic Obstructive Pulmonary Disease. *Am Rev Respir Dis* 147:1336–1340 (1993).
 37. Koenig, J.Q.; Larson, T.V.; Hanley, Q.S.; et al.: Pulmonary Function Changes in Children Associated with Fine Particulate Matter. *Environ Res* 63:26–38 (1993).
 38. Ozkaynak, H.; Thurston, G.D.: Associations Between 1980 U.S. Mortality Rates and Alternative Measures of Airborne Particle Concentration. *Risk Anal* 7:449–461 (1987).
 39. Lipfert, F.W.: Air Pollution and Mortality: Specification Searches Using SMSA-Based Data. *J Environ Econ Manage* 11:208–243 (1984).
 40. Dockery, D.W.; Pope, III, C.A.; Xu, X.; et al.: An Association Between Air Pollution and Mortality in Six U.S. Cities. *N Engl J Med* 329:1753–1759 (1993).
 41. Pope, C.A. III; Thun, M.J.; Namboodiri, M.M.; et al.: Particulate Air Pollution as a Predictor of Mortality in a Prospective Study of U.S. Adults. *Am J Respir Crit Care Med* 151:669–674 (1995).
 42. Euler, G.L.; Abbey, D.E.; Magie, A.R.; et al.: Chronic Obstructive Pulmonary Disease Symptom Effects of Long-Term Cumulative Exposure to Ambient Levels of Total Suspended Particulates and Sulfur Dioxide in California Seventh-Day Adventist Residents. *Arch Environ Health* 42:213–222 (1987).
 43. Dockery, D.W.; Speizer, F.E.; Stram, D.O.; et al.: Effects of Inhalable Particles on Respiratory Health of Children. *Am Rev Respir Dis* 139:587–594 (1989).
 44. Portney, P.R.; Mullahy, J.: Urban Air Quality and Chronic Respiratory Disease. *Regional Sci Urban Econ* 20:407–418 (1990).
 45. Schwartz, J.: Air Pollution and Hospital Admissions for the Elderly in Detroit, Michigan. *Am J Respir Crit Care Med* 150:648–655 (1994).
 46. Ostro, B.D.: The Effects of Air Pollution on Work Loss and Morbidity. *J Environ Econ Manage* 10:371–382 (1983).
 47. Ostro, B.D.: Air Pollution and Morbidity Revisited: A Specification Test. *J Environ Econ Manage* 14:87–98 (1987).
 48. Ostro, B.D.: Associations Between Morbidity and Alternative Measures of Particulate Matter. *Risk Anal* 10:421–427 (1990).
 49. Ostro, B.D.; Rothschild, S.: Air Pollution and Acute Respiratory Morbidity: An Observational Study of Multiple Pollutants. *Environ Res* 50:238–247 (1989).
 50. Ransom, M.R.; Pope, III, C.A.: Elementary School Absences and PM-10 Pollution in Utah Valley. *Environ Res* 58:204–219 (1992).

51. Schwartz, J.: Lung Function and Chronic Exposure to Air Pollution: A Cross-Sectional Analysis of NHANES II. *Environ Res* 50:309–321 (1989).
52. Raizenne, M.; Neas, L.; Damokosh, A.; et al.: Health Effects of Acid Aerosols on North American Children: Pulmonary Function. Paper Presented at the American Lung Association/American Thoracic Society International Conference, San Francisco, CA, May 16–19 (1993).
53. Chestnut, L.G.; Schwartz, J.; Savitz, D.A.; et al.: Pulmonary Function and Ambient Particulate Matter: Epidemiological Evidence from NHANES I. *Arch Environ Health* 46:135–144 (1991).
54. Dockery, D.W.; Damokash, A.I.; Neas, L.M.; et al.: Health Effects of Acid Aerosols on North American Children: Respiratory Symptoms and Illness. Presented at the American Lung Association/American Thoracic Society International Conference, San Francisco, CA, May 16–19 (1993).
55. Pope, Jr., C.A.; Dockery, D.W.; Schwartz, J.: Review of Epidemiological Evidence of Health Effects of Particulate Air Pollution. *Inhal Toxicol* 7:1–18 (1995).
56. Ozkaynak, H.; Thurston, G.D.: Associations Between 1980 U.S. Mortality Rates and Alternative Measures of Airborne Particle Concentration. *Risk Anal* 7:449–461 (1987).
57. Lippmann, M.: Background on Health Effects of Acid Aerosols. *Environ Health Perspect* 79:3–6 (1989).
58. Bates, D.V.; Sizto, R.: Air Pollution and Hospital Admissions in Southern Ontario: The Acid Summer Haze Effect. *Environ Res* 43:317–331 (1987).
59. Dockery, D.W.; Damokosh, A.I.; Neas, L.M.; et al.: Health Effects of Acid Aerosols on North American Children: Respiratory Symptoms and Illness. *Am Rev Respir Dis* 147:A633 (1993).
60. Ostro, B.D.; Lipsett, M.J.; Wiener, M.B.; et al.: Asthmatic Responses to Airborne Acid Aerosols. *Am J Public Health* 81:694–702 (1991).
61. Lippmann, M.; Ito, K.: Separating the Effects of Temperature and Season on Daily Mortality from Those of Air Pollution in London: 1965–1972. *Inhal Toxicol* 7:85–97 (1995).
62. Dockery, D.W.; Cunningham, J.; Damokosh, A.I.; et al.: Health Effects of Acid Aerosols on North American Children: Respiratory Symptoms. *Environ Health Perspect* 104:500–505 (1996).
63. Raizenne, M.; Neas, L.M.; Damokosh, A.I.; et al.: Health Effects of Acid Aerosols on North American Children: Pulmonary Function. *Environ Health Perspect* 104:506–514 (1996).
64. Environmental Protection Agency (EPA): Air Quality Criteria for Particulate Matter, Volume 1, EPA/600/P-95/001aF (1996).
65. Leikauf, G.D.; Spektor, D.M.; Albert, R.E.; et al.: Dose-Dependent Effects of Submicrometer Sulfuric Acid Aerosol on Particle Clearance from Ciliated Human Lung Airways. *Am Ind Hyg Assoc J* 45:285–292 (1984).
66. Spektor, D.M.; Yen, B.M.; Lippmann, M.: Effect of Concentration on Cumulative Exposure of Inhaled Sulfuric Acid on Tracheobronchial Particle Clearance in Healthy Humans. *Environ Health Perspect* 79:203–205 (1989).
67. Koenig, J.Q.; Pierson, W.E.; Horike, M.: The Effects of Inhaled Sulfuric Acid on Pulmonary Function in Adolescent Asthmatics. *Am Rev Respir Dis* 128:221–225 (1983).
68. Koenig, J.Q.; Covert, D.S.; Pierson, W.E.: Effects of Inhalation of Acidic Compounds on Pulmonary Function in Allergic Adolescent Subjects. *Environ Health Perspect* 79:173–178 (1989).
69. Utell, M.J.; Morrow, P.E.; Speers, D.M.; et al.: Airway Responses to Sulfate and Sulfuric Acid Aerosols in Asthmatics. An Exposure-Response Relationship. *Am Rev Respir Dis* 128:444–450 (1983).
70. Peters, A.; Dockery, D.W.; Heinrich, J.; et al.: Medication Use Modifies the Health Effects of Particulate Sulfate Air Pollution in Children with Asthma. *Environ Health Perspect* 105:2–7 (1997).
71. Peters, A.; Goldstein, I.F.; Beyer, U.; et al.: Acute Health Effects of Exposure to High Levels of Air Pollution in Eastern Europe. *Am J Epidemiol* 144:570–581 (1996).
72. Owen, M.K.; Ensor, D.S.; Hovis, L.S.; et al.: Particle Size Distributions for an Office Aerosol. *Aerosol Sci Technol* 13:486–492 (1990).
73. Owen, M.K.; Ensor, D.S.; Sparks, L.E.: Airborne Particle Sizes and Sources Found in Indoor Air. *Atmos Environ* 26A(12):2149–2162 (1992).
74. Kamens, R.; Lee, C.T.; Wiener, R.; et al.: A Study to Characterize Indoor Particles in Three Non-Smoking Homes. *Atmos Environ* 25(5/6):939–948 (1991).
75. Horstman, S.W.; Wagman, J.: Size Analysis of Acid Aerosols by a Metal Film Technique. *Am Ind Hyg Assoc J* 28:523–539 (1967).
76. Xiong, J.Q.; Zhong, M.; Fang, C.P.; et al.: Hygroscopicity of Fatty Acid Film Coated Ultrafine Sulfuric Acid Aerosol. *Environ Sci Technol* 32:3536–3541 (1998).
77. Binnig, G.; Rohrer, H.; Gerber, C.; et al.: Surface Studies by Scanning Tunneling Microscopy. *Phys Rev Lett* 49:57 (1982).
78. Howland, R.; Benatar, L.: A Practical Guide to Scanning Probe Microscopy, Park Scientific Instruments, Sunnyvale, CA 94089 (1996).